catalysts

MDPI

Article

Enhancement of Degradation and Dechlorination of Trichloroethylene via Supporting Palladium/Iron Bimetallic Nanoparticles onto Mesoporous Silica

Jianjun Wei *, Yajing Qian, Lutao Wang, Yijie Ge, Lingyan Su, Debin Zhai, Jiang Wang, Jing Wang and Jiang Yu

Department of Environmental Science and Engineering, Beijing University of Chemical Technology, Beijing 100029, China; jingjingq1216@163.com (Y.Q.); wanglutao1988@163.com (L.W.); ge.yijie@163.com (Y.G.); 764038015@163.com (L.S.); youshangdeyouxiang@foxmail.com (D.Z.); jims_wang@smics.com (J.W.); wangjing649@163.com (J.W.); yujiang@mail.buct.edu.cn (J.Y.)

* Correspondence: weijj@mail.buct.edu.cn; Tel.: +86-137-1773-6109

Academic Editor: John R. (JR) Regalbuto

Received: 15 March 2016; Accepted: 24 June 2016; Published: 19 July 2016

Abstract: This study is aimed to prevent the agglomeration of Pd/Fe bimetallic nanoparticles and thus improve the efficiency toward degradation and dechlorination of chlorinated organic contaminants. A mesoporous silica with a primary pore diameter of 8.3 nm and a specific surface area of 688 m^2/g was prepared and used as the host of Pd/Fe nanoparticles. The Pd/Fe nanoparticles were deposited onto or into the mesoporous silica by reduction of ferrous ion and hexachloropalladate ion in aqueous phase. Batch degradation and dechlorination reactions of trichloroethylene were conducted with initial trichloroethylene concentration of 23.7 mg/L, iron loading of 203 or 1.91 $\times$ 10^3 mg/L and silica loading of 8.10 g/L at 25 °C. Concentration of trichloroethylene occurs on the supported Pd/Fe nanoparticles, with trichloroethylene degrading to 56% and 59% in 30 min on the supported Pd/Fe nanoparticles with weight percentage of palladium to iron at 0.075% and 0.10% respectively. The supported Pd/Fe nanoparticles exhibit better dechlorination activity. When the supported Pd/Fe nanoparticles with a weight percentage of palladium to iron of 0.10% were loaded much less than the bare counterpart, the yield of ethylene plus ethane in 10 h on them was comparable, i.e., 19% vs. 21%. This study offers a future approach to efficiently combine the reactivity of supported Pd/Fe nanoparticles and the adsorption ability of mesoporous silica.

Keywords: Pd/Fe bimetallic nanoparticles; mesoporous silica; trichloroethylene; adsorption; concentration; degradation; dechlorination

1. Introduction

Bimetallic iron nanoparticles such as palladium/iron (Pd/Fe) and nickel-iron (Ni-Fe) nanoparticles have been proven to be effective in transforming chlorinated organic contaminants in groundwater or wastewater into innocuous or biodegradable compounds [1–6]. For example, catalytic dechlorination of aqueous trichloroethylene by Pd/Fe nanoparticles can be expressed by Equation (1). If n equals 4, then trichloroethylene is converted into ethane; if n equals 3, then ethylene is produced. Iron mediates the reductive dechlorination providing electrons, water donates hydrogen, and palladium acts as a catalyst initiating the reaction.

$$C_2HCl_3 + nFe + (2n-3)H_2O \overset{Pd}{\rightleftharpoons} C_2H_{2n-2} + nFe^{2+} + 3Cl^- + (2n-3)OH^- \quad (1)$$

Pd/Fe nanoparticles tend to agglomerate due to high surface energy and magnetic attraction, decreasing the specific surface area and hence lowering dechlorination activity. Immobilizing Pd/Fe

nanoparticles into solid hosts is a preferable way to overcome the deficiency. The dispersion of Pd/Fe nanoparticles can be improved through the immobilization; therefore, more surface sites of iron and palladium will be provided, giving more reductive hydrogen species. Furthermore, contaminant molecules adsorbed into the porous hosts can get easier access to the nanoparticles. As a result, the reaction rate will be enhanced. In this regard, different materials, such as carbon [7–9] and silica [10,11], have been evaluated. It has been shown that degradation ratio of dichromate is enhanced on a composite of silica fume and iron nanoparticles relative to bare iron nanoparticles [10]. Adsorption and dechlorination of 2-chlorobiphenyl occur simultaneously on a composite of Pd-Fe nanoparticles and activated carbon [7]. Adsorption and dechlorination happen consecutively on iron nanoparticles/carbon and Pd/Fe nanoparticles/ethyl-silica [8,9,11], during which much more rapid adsorption than dechlorination means concentration of trichloroethylene molecules into the host.

An interesting feature of silica materials is the surface silanol groups. Metal cations can be adsorbed onto the negatively charged surface of silica through electrostatic force at pH values above its point of zero charge, which makes it possible to obtain highly dispersed metal nanoparticles inside the pores of silica materials. The use of mesoporous silicas with pore diameters ranging approximately from 2 to 50 nm as hosts of iron nanoparticles has attracted interest in the area of groundwater remediation due to the need to enhance the efficiency of iron nanoparticles. Indeed, since the report of synthesis of MCM-41 in 1992 [12], mesoporous silicas have been researched on the subjects of catalysis [13], drug and gene delivery [14], etc., because of their large specific surface area, tunable pore size, great porosity and suitability for surface functionalization. For example, SBA-15 mesoporous silica materials have been reported to possess BET (Brunauer-Emmett-Teller) specific surface areas of 690–1040 m^2/g, pore sizes of 4.6–30 nm and pore volumes up to 2.5 cm^3/g [15]. The capacities of iron nanoparticles supported on mesoporous silicas for degrading decabromodiphenyl ether, nitrobenzene and dichromate have been evaluated. Degradation percentage of decabromobiphenyl ether by iron nanoparticles immobilized in mesoporous silica is greater by 1.4 times than the unsupported iron nanoparticles [16]. Iron nanoparticles supported on mesoporous silica SBA-15 exhibit greater degradation and conversion ratio for nitrobenzene than the bare counterpart [17]. Iron nanoparticles immobilized in mesoporous silica show enhanced degradation ratio for dichromate compared to the bare counterpart [18].

In this study, degradation and dechlorination of trichloroethylene by Pd/Fe nanoparticles was enhanced via immobilizing the nanoparticles into mesoporous silica. Mesoporous silica was prepared with the addition of pore-expanding agent, and the pore size distribution and BET specific surface area were measured. The Pd/Fe bimetallic nanoparticles were supported onto the mesoporous silica by reduction of ferrous iron with sodium borohydride and then deposition of palladium onto the surface of iron nanoparticles in the presence of the host. A lower weight percentage of iron to mesoporous silica (2.50%) than that of the references mentioned is employed to better show the enhancement of accessibility of the Pd/Fe nanoparticles to trichloroethylene molecules, because large weight percentage of nanoparticles may result in partial blockage of pores and thus inaccessibility of some nanoparticles. The immobilization of the nanoparticles into the host was examined by TEM (transmission electron microscopy). The rate of degradation and dechlorination of trichloroethylene by the Pd/Fe nanoparticles supported on mesoporous silica and the bare counterpart were compared to demonstrate the remarkable positive effect of the immobilization.

2. Results

2.1. Physical Characterization

No peaks characteristic of ordered mesoporous silica can be found on the low-angle XRD (X-ray powder diffraction) pattern of the mesoporous silica, as shown in Figure A1. It indicates that the mesoporous silica with expanded pores is amorphous. This feature is also illustrated by the irregular arrangement of mesopores on the TEM image of Figure A2.

The nitrogen adsorption-desorption isotherm of mesoporous silica is shown in Figure 1a. The isotherm shows the characteristic hysteresis loop of mesoporous materials, which is associated with capillary condensation taking place in mesopores [19]. The range of the hysteresis loop is wider than that of a mesocellular siliceous foam [20], indicating a wider pore size distribution. Indeed, as shown in Figure 1b, the pore diameters peak at 4.0, 6.9, 8.3 and 10.3 nm with the primary diameter at 8.3 nm; and the pore diameters mainly range between 4.5 and 18.4 nm. The mesoporous silica has a BET specific surface area of 688 m^2/g and a specific pore volume of 1.46 cm^3/g. Similarly, the mesocellular siliceous foam [20] possesses a BET specific surface area of 655 m^2/g and a specific pore volume of 1.7 cm^3/g.

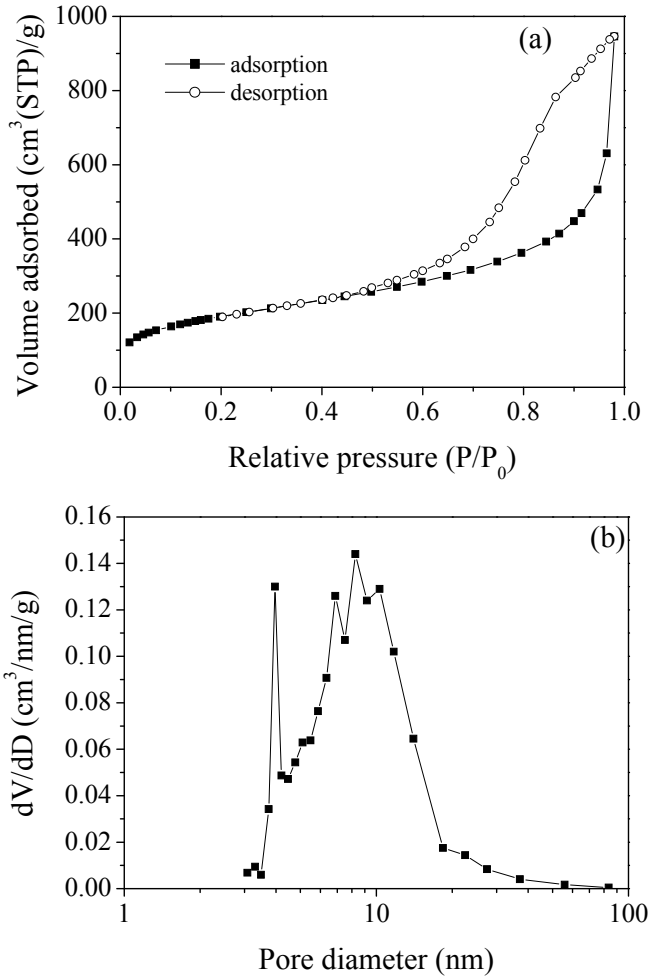

Figure 1. Nitrogen adsorption-desorption isotherm (**a**) and BJH (Barrett-Joyner-Halenda) pore size distribution curve (**b**) of mesoporous silica. STP means standard temperature and pressure, and *D* means diameter.

The wide-angle XRD pattern of the Pd/Fe nanoparticles supported on mesoporous silica is displayed in Figure 2. Only a broad peak ranging from 15° to 30°, which is ascribed to amorphous silica [17], can be observed. The lack of diffraction peaks of iron and palladium is caused by their low percentages to the host, i.e., 2.50 wt. % and 0.0019 wt. % respectively.

Figure 3 shows the TEM images of bare Pd/Fe nanoparticles and Pd/Fe nanoparticles supported on mesoporous silica. Bare Pd/Fe nanoparticles are agglomerated together, as can be seen in Figure 3a. Well defined and scattered nanoparticles with petal-like shell in diameters of about 50–100 nm are immobilized into the mesoporous silica, as shown in Figure 3b,c. Pd/Fe nanoparticles appear in black and silica walls in gray due to electronic density contrast. The relatively thin particles are especially

characteristic of the immobilization of Pd/Fe nanoparticles into the host. The results demonstrate that dispersion of Pd/Fe nanoparticles can be achieved by immobilizing them into mesoporous silica.

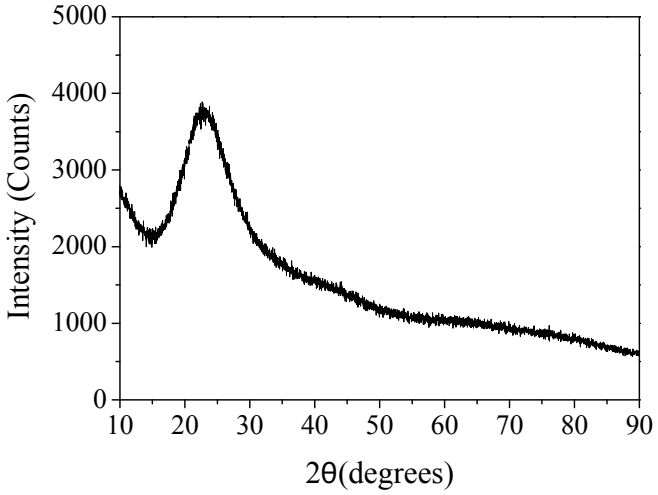

Figure 2. Wide-angle XRD pattern of Pd/Fe nanoparticles supported on mesoporous silica. Weight percentage of iron to silica is 2.50%, and weight percentage of Pd to Fe is 0.075%.

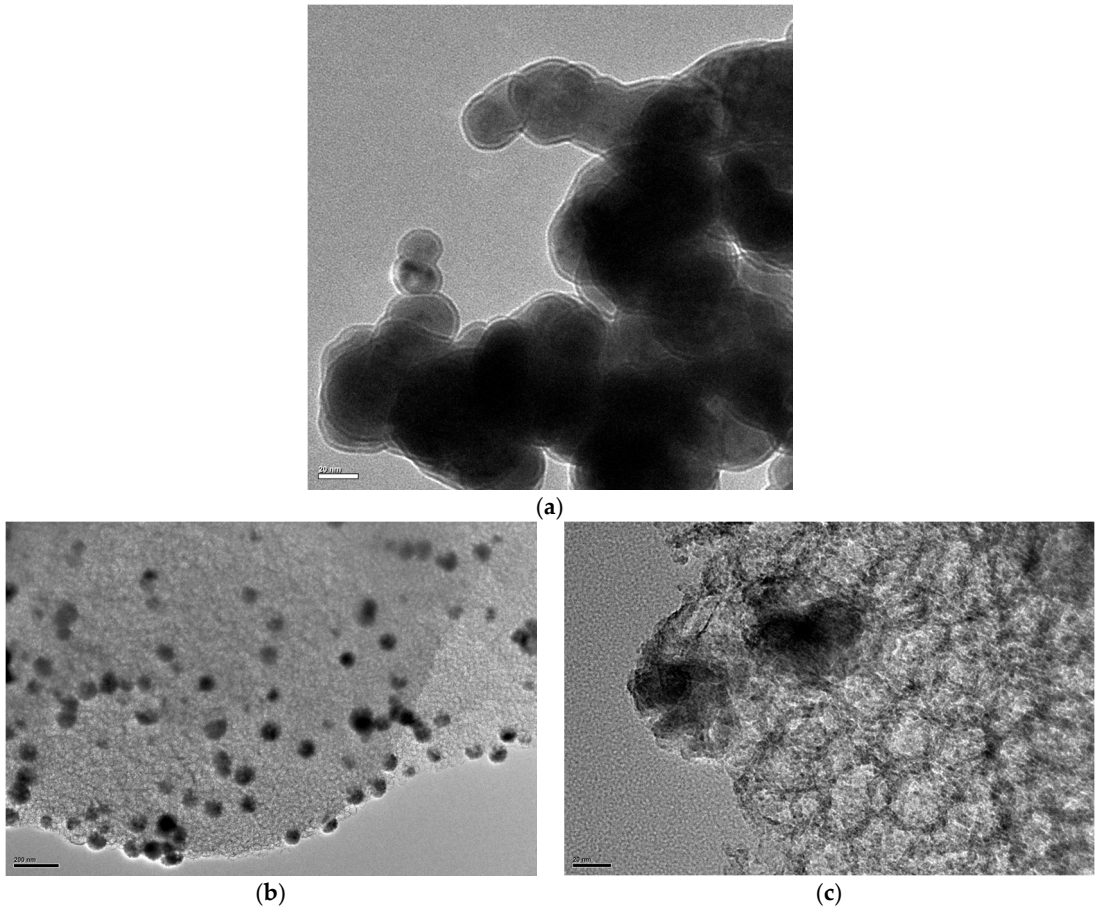

Figure 3. TEM images of bare Pd/Fe nanoparticles (**a**), and Pd/Fe nanoparticles supported on mesoporous silica (**b**,**c**). The scale bars are 20 nm (**a**,**c**), and 200 nm (**b**). A bare Pd/Fe nanoparticles with weight percentage of Pd to Fe at 0.30% is examined. For the supported Pd/Fe nanoparticles, weight percentage of iron to silica is 2.50%, and weight percentage of Pd to Fe is 0.075%.

2.2. Enhancement of Degradation and Dechlorination of Trichloroethylene

As shown in Figure 4a, the amount of trichloroethylene degrades to 79% of the initial value in 10 h on the mesoporous silica; and it degrades to 64% in a same period by the bare Pd/Fe nanoparticles. In comparison, much greater trichloroethylene degradation is achieved by the Pd/Fe nanoparticles supported on mesoporous silica, with 34% of the initial trichloroethylene being left in 10 h. It is noteworthy that a plunge occurs within the initial half hour on the Pd/Fe nanoparticles supported on mesoporous silica, as shown by the red circle in Figure 4a, indicating that the supported Pd/Fe nanoparticles has the ability to attract trichloroethylene rapidly. The yield of ethylene is 1.5% and 3.9% in 8 h on the supported and bare Pd/Fe nanoparticles respectively; meanwhile ethane is produced by 10% and 2.7% respectively, as shown in Figure 4b,c. Therefore, the total yield of ethylene and ethane is 12% in 8 h on the supported Pd/Fe nanoparticles, compared to 6.6% on the bare counterpart, as shown in Figure 4d. The yield of ethylene reaches a stage in 2 h on the supported Pd/Fe nanoparticles. However, it keeps increasing on the bare counterpart within 10 h. Since ethylene is the intermediate product, it indicates that more rapid conversion of ethylene into ethane occurs on the supported Pd/Fe nanoparticles. The results indicate that immobilizing Pd/Fe nanoparticles onto the host is favorable to degradation and dechlorination of trichloroethylene.

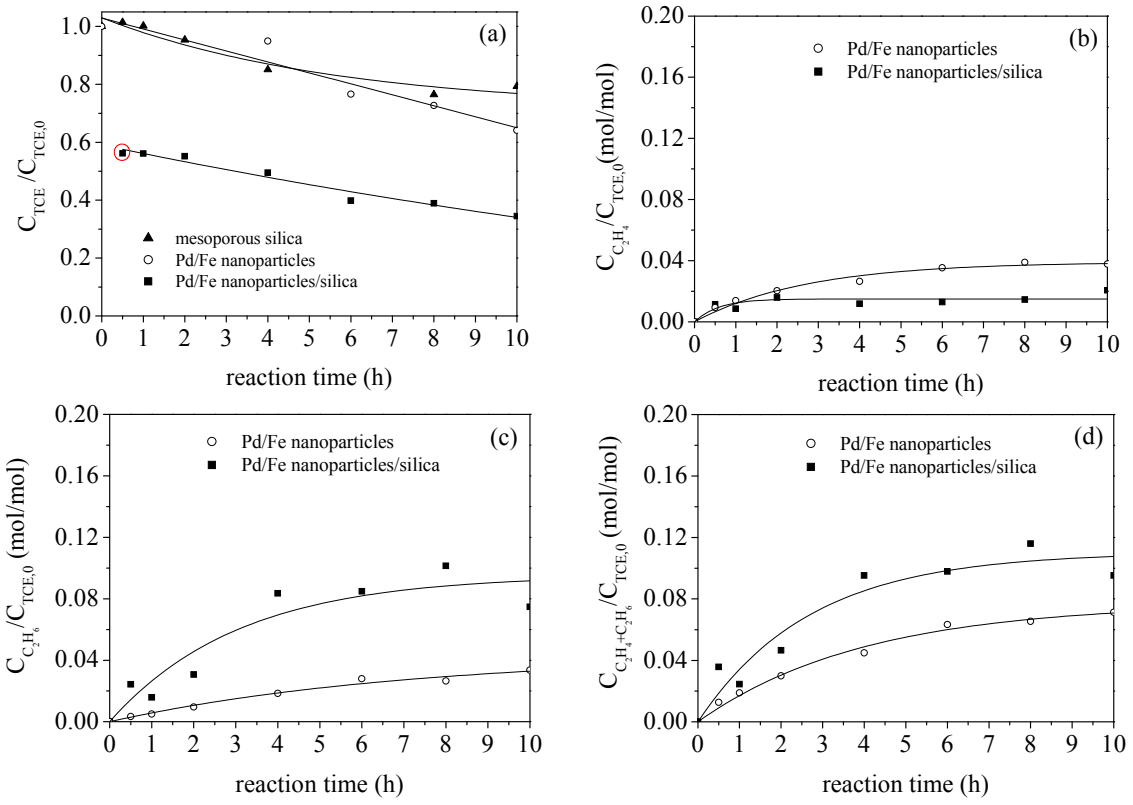

Figure 4. Degradation of trichloroethylene (**a**), and production of ethylene (**b**), ethane (**c**) and ethylene plus ethane (**d**) on bare Pd/Fe nanoparticles and Pd/Fe nanoparticles supported on mesoporous silica with a same weight percentage of Pd to Fe at 0.075%, also shown in (**a**) is trichloroethylene degradation on mesoporous silica. TCE refers to trichloroethylene and silica refers to mesoporous silica. $C_{TCE,0}$ = 23.7 mg/L (0.181 mmol/L), iron loading = 203 mg/L (3.63 mmol/L), and for the mesoporous silica and the supported Pd/Fe nanoparticles, mesoporous silica loading = 8.10 g/L.

In order to make it clear that the availability of Pd/Fe nanoparticles can be enhanced dramatically via the immobilization into the host, supported Pd/Fe nanoparticles with a weight percentage of palladium to iron at 0.10% were loaded at five times the stoichiometric amount of iron needed

to transform trichloroethylene into ethane, whereas the corresponding bare Pd/Fe nanoparticles was loaded at 47 times. Figure 5 presents the comparison between them. Gradual degradation of trichloroethylene and gradual production of ethylene plus ethane are observed for the bare Pd/Fe nanoparticles, with 32% of the initial trichloroethylene remaining and ethylene plus ethane being produced by 21% in 10 h. Although the supported Pd/Fe nanoparticles are employed at a much smaller iron loading than the bare counterpart, trichloroethylene plunges to 32% of the initial amount in 1 h on it. This value is equivalent to that in 10 h on the bare Pd/Fe nanoparticles. Accordingly, the production of ethylene plus ethane are more rapid within the first one hour on the supported Pd/Fe nanoparticles, the overall yield of ethylene and ethane reaches 17% in 1 h, compared to 7.6% on the bare counterpart. Subsequently, the amount of trichloroethylene and the products do not exhibit considerable decreasing and increasing trend, with trichloroethylene degrading to 28% and ethylene plus ethane being produced by 19% in 10 h. The overall yield of ethylene plus ethane in 10 h on the supported Pd/Fe nanoparticles is close to that on the bare counterpart. Considering that the supported Pd/Fe nanoparticles are loaded much less than the bare counterpart, it indicates that the availability of Pd/Fe nanoparticles for dechlorination reaction is improved via immobilizing them onto mesoporous silica.

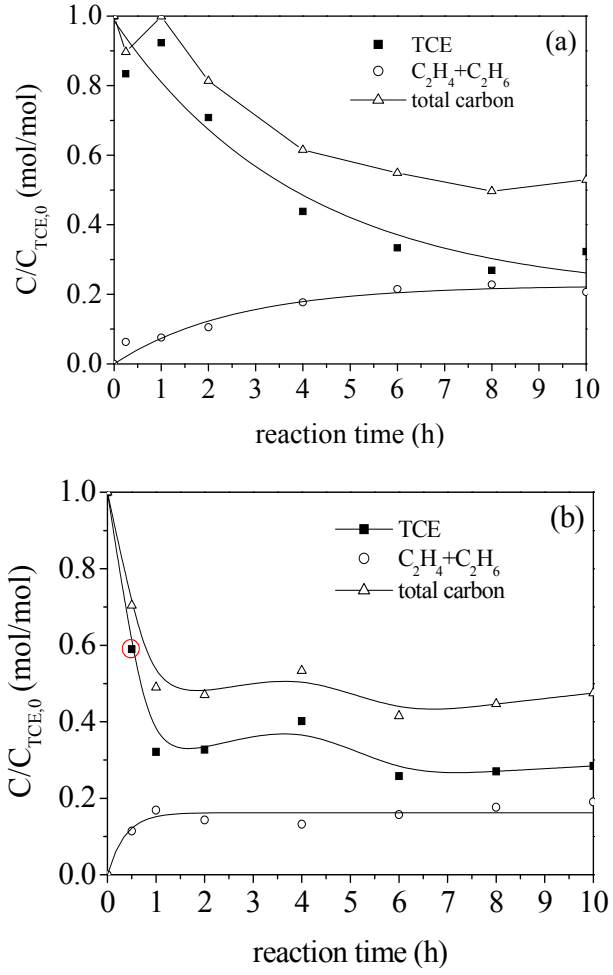

Figure 5. Degradation of trichloroethylene, and production of ethylene plus ethane on bare Pd/Fe nanoparticles (**a**) and Pd/Fe nanoparticles supported on mesoporous silica (**b**) with a same weight percentage of Pd to Fe at 0.10%. For the bare Pd/Fe nanoparticles, $C_{TCE,0}$ = 23.7 mg/L (0.181 mmol/L), iron loading = 1.91×10^3 mg/L (34.2 mmol/L). For the supported Pd/Fe nanoparticles, $C_{TCE,0}$ = 23.7 mg/L (0.181 mmol/L), iron loading = 203 mg/L (3.63 mmol/L), mesoporous silica loading = 8.10 g/L.

3. Discussion

3.1. Pore Structure and Dispersion of Pd/Fe Nanoparticles

Since pore-expanding step was introduced into the preparation of mesoporous silica and the aging step was carried out at ambient pressure, non-crystalline morphology with ununiform pore size was obtained. The primary diameter of 8.3 nm is smaller than that obtained by Schmidt-Winkel et al. [20] with the same preparation conditions except for the aging step, which is a monodispersed size of 11 nm. The primary diameter is greater than that of 6.0 nm in reference [21], which employs a same preparation method except that the addition of 1,3,5-methylbenzene was skipped and the aging step was performed in sealed Teflon flask. The larger pore sizes obtained in this study are attributed to the addition of pore-expanding agent (1,3,5-trimethylbenzene) at the high hydrolysis temperature (40 °C). This temperature is beneficial to the diffusion of 1,3,5-trimethylbenzene into the hydrophobic PPO (poly(propylene oxide)) core of Pluronic P123 micelles [22], which results in pore expansion. Larger mesopore sizes are favorable to the growth of Pd/Fe nanoparticles in the host. The mesoporous silica has a BET specific surface area of 688 m^2/g and a specific pore volume of 1.46 cm^3/g, which are comparable to the values of the mesocellular siliceous foam [20]. By comparison with the specific pore volume of 0.86 cm^3/g in reference [21], it is obvious that the specific pore volume has been greatly enhanced by the pore-expansion step. In application, the host can also act as an adsorption material and thus a collector for contaminants. The collected contaminant molecules can gain easier access to the immobilized Pd/Fe nanoparticles than those dissolved in aqueous phase.

As shown in Figure 3b,c, the supported Pd/Fe nanoparticles are larger than the pore diameter of the mesoporous silica because they are supported on the outer surface of the host or have grown across the silica walls through the micropores on the walls. Taghavimoghaddam et al. [21] and Sun et al. [18] have demonstrated the formation of cobalt oxide nanoparticles and iron nanoparticles inside the pores of mesoporous silica. Since dechlorination of trichloroethylene occurs on the surface of Pd/Fe nanoparticles, large specific surface area would be desirable. The dispersion of the supported Pd/Fe nanoparticles provides them with larger specific surface area and thus greater dechlorination activity than the bare counterpart. The observation by TEM demonstrates that mesoporous silica is a preferable host for Pd/Fe nanoparticles.

3.2. Enhancement of Degradation and Dechlorination of Trichloroethylene

No degradation of trichloroethylene is observed in 30 min for both mesoporous silica and the bare Pd/Fe nanoparticles with weight percentage of palladium to iron at 0.075% (Figure 4a). And only a degradation of 17% is observed in 15 min on the bare Pd/Fe nanoparticles with weight percentage of palladium to iron at 0.10% (Figure 5a). However, trichloroethylene does plunge to 56% and 59% in 30 min on the Pd/Fe nanoparticles supported on mesoporous silica with weight percentage of palladium to iron at 0.075% and 0.10% respectively, as shown by the red circles in Figures 4a and 5b. Besides, Pd/Fe nanoparticles supported on mesoporous silica with weight percentage of palladium to iron at 0.050% also exhibit a similar plunge, as shown in Figure A3. The greater degradation of trichloroethylene in the initial phase of the reaction on the supported Pd/Fe nanoparticles is attributed to the immobilization effect. The plunge of aqueous concentration of trichloroethylene implies the collection of organic contaminants from aqueous media and even a driving force for dissolution of dense non-aqueous phase liquid in groundwater before it being degraded. Plunge of amount of reactants within the initial phase of degradation on iron nanoparticles immobilized into mesoporous silica [17,18], carbon [8] and silica [11] has also been observed. The concentration of trichloroethylene molecules into the Pd/Fe nanoparticles supported on mesoporous silica gives them much easier access to the immobilized Pd/Fe nanoparticles than to the bare counterpart. Moreover, the immobilized Pd/Fe nanoparticles are dispersed and thus can provide more available surface sites than the bare counterpart. As a result, the immobilized Pd/Fe nanoparticles exhibit better dechlorination activity than the bare counterpart. The overall yield of ethylene plus ethane in 8 h on the supported Pd/Fe

nanoparticles with weight percentage of palladium to iron of 0.075% (12%) is greater than that on the bare counterpart (6.6%). Furthermore, the production of ethylene predominates on the bare Pd/Fe nanoparticles, it comprises 59% of the products in 8 h; whereas the production of ethane predominates on the supported Pd/Fe nanoparticles, it comprises 87% of the products in a same period. Iron plays the role of mediator and palladium serves as the catalyst, as described in Section 1. Lien et al. [23] have proven that palladium, as the catalyst, does not change and iron is oxidized during the dechlorination reaction. Furthermore, galvanic cell process is involved in the reaction happening on the bimetallic nanoparticles [24], as shown by the schematic diagram in Figure 6. Iron is the anode and palladium is the cathode. Protons are reduced by the electrons transferred from iron to form highly active atomic hydrogen (H*) and hydrogen gas (H_2) on the surface of palladium. Trichloroethylene molecules adsorbed on the palladium sites are reduced to ethylene and then ethane by the active atomic hydrogen. Two steps are involved in the dechlorination reaction. Firstly trichloroethylene is converted into ethylene via hydrogenolysis, which results from the dissociation of carbon-chlorine bond and the formation of carbon-hydrogen bond on palladium surface [23]. Then ethylene is hydrogenated to produce ethane. Greater overall yield and greater ethane percentage in the products on the supported Pd/Fe nanoparticles definitely demonstrate that the supported Pd/Fe nanoparticles can provide more surface sites of iron and palladium and generate more active atomic hydrogen. Figure 3a shows us that bare Pd/Fe nanoparticles are agglomerated severely and thus cannot be utilized efficiently. Even when the supported Pd/Fe nanoparticles with the weight percentage of palladium to iron at 0.10% were loaded much less than the bare counterpart, the former still exhibits better performance than the latter, as described in Section 2.2. The results indicate that Pd/Fe nanoparticles supported on mesoporous silica are more efficient for degradation and dechlorination of trichloroethylene. This study suggests that mesoporous silica is a preferable host for Pd/Fe nanoparticles used for abatement of aqueous chlorinated organic contaminants.

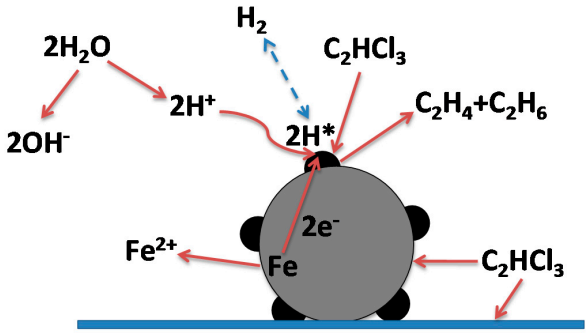

Figure 6. Schematic diagram of Pd/Fe galvanic cell process, the grey ball is an iron nanoparticle, the black balls are tiny palladium particles, and the horizontal bar represents silica wall. The standard reduction potential of Fe^{2+}/Fe and Pd^{2+}/Pd pair is −0.447 and 0.951 V respectively [23].

Degradation of trichloroethylene is greater than production of ethylene plus ethane in all cases. Four factors leads to the difference, i.e., passivation of the surface of Pd/Fe nanoparticles, loss of palladium, competition for the catalyst sites between trichloroethylene molecules and protons, and unavailability of some trichloroethylene molecules. First of all, iron is oxidized to mediate the reductive dechlorination, giving ferrous ions; and because the amount of water is much more than that of trichloroethylene, much more ferrous ions are produced to generate hydrogen gas, as shown in Figure 6. Subsequently, ferrous ions combine with hydroxide ions to form ferrous hydroxide. And when air exists in the reactors, goethite and lepidocrocite, which are both in formula of FeOOH, can also form. The (oxi)-hydroxides will precipitate onto the surface of the Pd/Fe nanoparticles, and accumulation of precipitates will lead to passivation of the nanoparticles. The passivation layer may even cover the adsorbed trichloroethylene molecules. Secondly, the tiny particles of palladium may be dislodged due to the oxidation of iron around them, i.e., the catalyst particles may be lost.

Thirdly, protons compete with trichloroethylene molecules for the sites of palladium. Because of the low concentration of trichloroethylene in water, a much larger amount of hydrogen gas is generated than the products. When the hydrogen pressure in reactor headspace is large enough, the conversion of trichloroethylene into gaseous ethylene and ethane may be inhibited. Fourthly, headspace samples were analyzed to obtain trichloroethylene concentration in the liquid phase according to Henry's law. It means that some trichloroethylene cannot contribute to the transformation. Furthermore, some trichloroethylene molecules remain adsorbed on non-reactive sites of iron and mesoporous silica or covered under the passivation layer in 10 h and thus are also not available for dechlorination. Consequently, the yield of ethylene plus ethane is much less than the degradation percentage of trichloroethylene. Besides, the deactivation, i.e., the first three factors, progresses more rapidly on the supported Pd/Fe nanoparticles. As a result, the production of ethylene plus ethane reaches a stage earlier on the two supported Pd/Fe nanoparticles, as shown in Figures 4d and 5. Figures 7 and 8 show the morphology of the reacted bare and supported Pd/Fe nanoparticles. Porous particles, and platelets which are horizontal or vertical, are observed on Figure 7 for the reacted bare Pd/Fe nanoparticles. Porous particles are formed by oxidation of iron and loss of palladium and their surface bears tiny precipitation particles. Platelets are probably to be goethite or lepidocrocite phase. The previous Pd/Fe nanoparticles that were supported on the mesoporous silica disappear after reaction with trichloroethylene for 34 h, as indicated by TEM observation (Figure 8). The spot in the white circle only contains 28.50% of iron by weight. It demonstrates that the oxidation of iron and the disintegration of the bimetallic nanoparticles have taken place during the reaction. The carbon recovery ranges from 44% to 60%, and 42% to 70% within 10 h for the Pd/Fe nanoparticles supported on mesoporous silica with weight percentage of palladium to iron at 0.075% and 0.10% respectively. And it ranges from 71% to 100%, and 50% to 100% for the bare Pd/Fe nanoparticles with weight percentage of palladium to iron at 0.075% and 0.10% respectively. Future research is needed to develop Pd/Fe nanoparticles supported on mesoporous silica with greater Pd/Fe content to better combine the adsorption ability of the host and the dechlorination activity of the bimetallic nanoparticles.

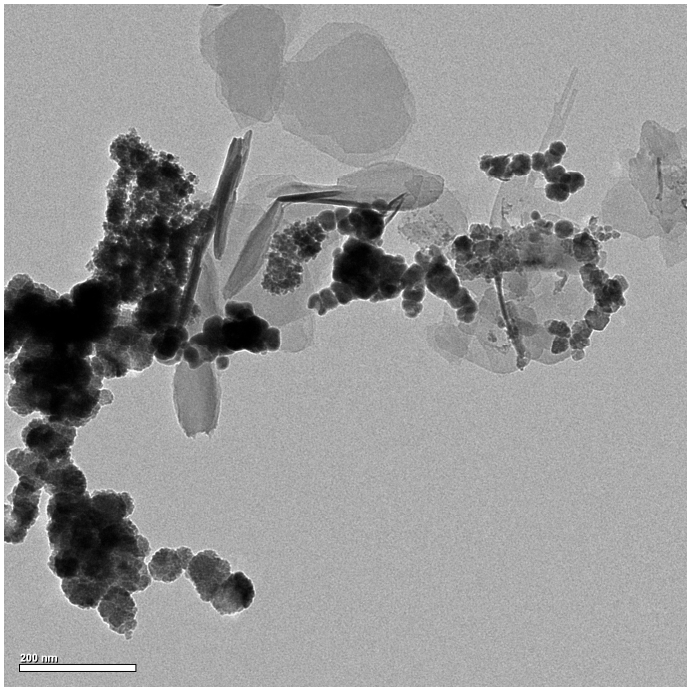

Figure 7. TEM image of bare Pd/Fe nanoparticles that have reacted with trichloroethylene for 10 h. The weight percentage of Pd to Fe is 0.30%, $C_{TCE,0}$ = 23.7 mg/L (0.181 mmol/L), iron loading = 1.91×10^3 mg/L (34.2 mmol/L).

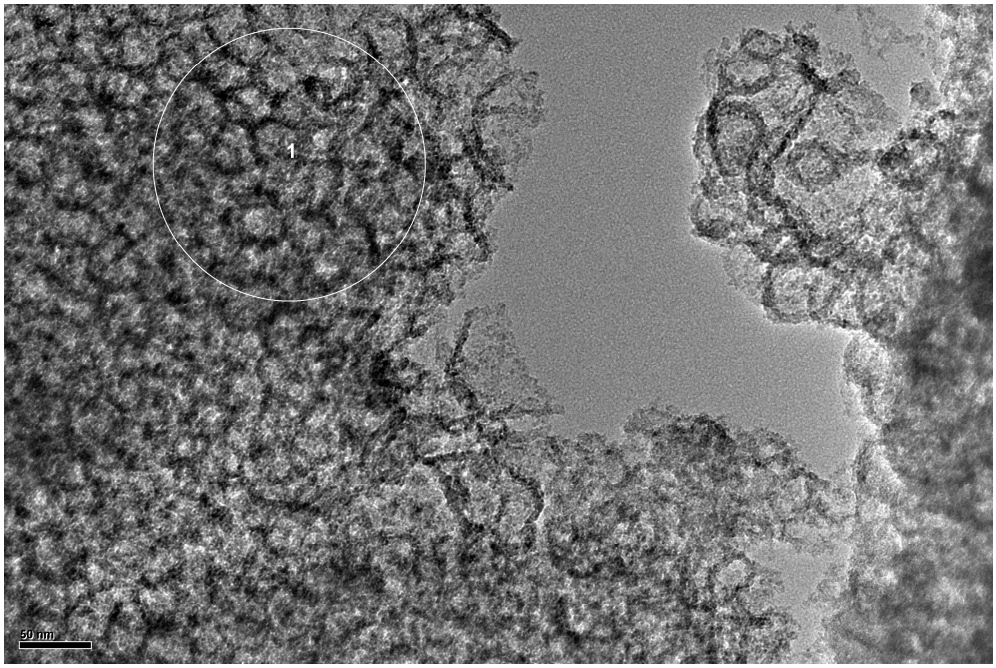

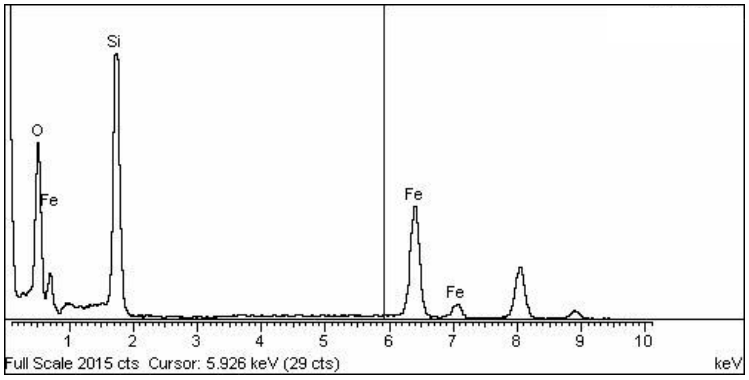

Element	Weight%
O-K	33.80
Si-K	37.70
Fe-K	28.50
Total	100.00

Figure 8. TEM image and TEM-EDS (transmission electron microscopy-energy dispersive spectroscopy) spectrum of Pd/Fe nanoparticles supported on mesoporous silica that have reacted with trichloroethylene for 34 h. The weight percentage of Pd to Fe is 0.075%, $C_{TCE,0}$ = 23.7 mg/L (0.181 mmol/L), iron loading = 203 mg/L (3.63 mmol/L), mesoporous silica loading = 8.10 g/L.

4. Materials and Methods

4.1. Materials

Tetraethyl orthosilicate (⩾28.4% in terms of silica), 1,3,5-trimethylbenzene (⩾99.9%), ferrous sulfate heptahydrate ($FeSO_4 \cdot 7H_2O$, 99.0%–101.0%), sodium borohydride ($NaBH_4$, 96%), trichloroethylene (⩾99.0%) and methanol (99.5%) were purchased from Sinopharm Chemical Reagent Beijing Co. Ltd. (Beijing, China). Pluronic P123 ($EO_{20}PO_{70}EO_{20}$, average molecular weight is 5800) and potassium hexachloropalladate (K_2PdCl_6, 99%) were bought from Sigma-Aldrich (Steinheim, Germany and St Louis, MO, USA). Ethane and ethylene reference gases were purchased from Huayuan Gas Chemical Industry Co. Ltd. (Beijing, China). Hydrochloric acid (36.0%–38.0%) was from Beijing Organic Chemical Works (Beijing, China). All experiments were conducted using pure water. Stock solution of trichloroethylene at 497 mg/L (3.79 mmol/L) was prepared by dissolving a 34 μL of trichloroethylene in a 2 mL of methanol and then diluting the solution with water in a 100 mL volumetric bottle. Stock solution of K_2PdCl_6 at 0.5 mg/mL was prepared in dilute hydrochloric acid of 0.01 mol/L.

4.2. Methods

4.2.1. Preparation of Mesoporous Silica

Mesoporous silica was prepared following the method reported by Schmidt-Winkel et al. [20] except that the aging step was performed at the boiling point of water and ambient pressure. First, a 4 g of Pluronic P123 was stirred into a 150 mL of 1.9 mol/L hydrochloric acid at 40 °C. Since Pluronic P123 has both hydrophilic poly(ethylene oxide) (PEO) chains and hydrophobic poly(propylene oxide) (PPO) chains, micelles were formed with PPO as the core and PEO as the corona. To this solution, a 6 g of 1,3,5-trimethylbenzene, which acted as the pore expanding agent, was added and diffused into the core of the micelles via stirring for 2 h. Afterwards, an 8.5 g of tetraethyl orthosilicate was added dropwise. Tetraethyl orthosilicate hydrolyzed and condensed around the surfactant micelles for 20 h under stirring at 40 °C. Then the sol was aged at the boiling point of water and ambient pressure for 24 h. The solid product was filtrated, washed and then dried in air. It was finally calcined in a muffle oven at 500 °C for 6 h after increasing the temperature from room temperature to 500 °C at a ramp rate of 1 °C/min.

4.2.2. Preparation of Pd/Fe Nanoparticles Supported on Mesoporous Silica and Bare Pd/Fe Nanoparticles

Pd/Fe nanoparticles supported on mesoporous silica with weight percentages of palladium to iron at 0.075% and 0.10% were prepared. The weight percentage of iron to silica was 2.50%. In the preparation of the supported Pd/Fe nanoparticles with a weight percentage of palladium to iron at 0.10%, a 0.317 g (1.14 mmol) of $FeSO_4 \cdot 7H_2O$ which was dissolved in a 30 mL of water, and a 0.48 mL of stock solution of K_2PdCl_6 (0.24 mg of K_2PdCl_6) were mixed with a 150 mL of aqueous suspension containing a 2.55 g of mesoporous silica which had been boiled in water for 2 h to re-generate surface silanol groups. Ferrous ion was adsorbed onto the surface of mesoporous silica via ion exchange. A 0.104 g (2.75 mmol) of solid $NaBH_4$ was then gradually added into the mixture under stirring to produce Pd/Fe nanoparticles supported on mesoporous silica. The reactions are expressed by Equations (2) and (3). The as-prepared Pd/Fe nanoparticles supported on mesoporous silica were diluted into a 300 mL of aqueous suspension before reaction with trichloroethylene.

$$Fe^{2+}/SiO_2 + 2BH_4^- + 6H_2O \rightarrow Fe/SiO_2 + 7H_2\,(g) + 2B\,(OH)_3 \quad (2)$$

$$(n\mathrm{Fe})/SiO_2 + PdCl_6^{2-} \rightarrow 2Fe^{2+} + Pd/(n-2)Fe/SiO_2 + 6Cl^- \quad (3)$$

Bare Pd/Fe nanoparticles with a weight percentage of palladium to iron of 0.075% were prepared by the same method mentioned above except for the addition of the host. Bare Pd/Fe nanoparticles with a weight percentage of palladium to iron at 0.10% was prepared by reduction of a 2.00 g (7.19 mmol) of $FeSO_4 \cdot 7H_2O$ with a 0.58 g (15 mmol) of $NaBH_4$, followed by reductive deposition of palladium from a 3.00 mL of stock solution of K_2PdCl_6 (1.50 mg of K_2PdCl_6). The resultant nanoparticles were washed three times with water after each reduction step. The as-prepared bare Pd/Fe nanoparticles were diluted into a 200 mL of aqueous suspension before reaction with trichloroethylene.

4.2.3. Characterization of Mesoporous Silica, Pd/Fe Nanoparticles Supported on Mesoporous Silica and Bare Pd/Fe Nanoparticles

Structural characteristics of the mesoporous silica and the Pd/Fe nanoparticles supported on mesoporous silica were determined with an X-ray powder diffractometer (D8 Advance, Bruker AXS, Karlsruhe, Germany) utilizing Cu Kα_1 radiation (λ = 1.54056 Å). The Pd/Fe nanoparticles supported on mesoporous silica was dried in a Schlenk line before the analysis. The nitrogen adsorption-desorption isotherm of the mesoporous silica was obtained on a specific surface area and pore size analyzer (NOVA 4200e, Quantachrome, Boynton Beach, FL, USA). The particles were outgassed at 200 °C for 2 h prior to

the analysis. The pore size distribution was calculated from the desorption branch of the isotherm using the BJH model. The pore volume was measured at the relative pressure of 0.98. The specific surface area was obtained using the BET method over the relative pressure range of 0.034–0.198. The morphology of the bare and supported Pd/Fe nanoparticles was observed on transmission electron microscopes (Tecnai 20, PHILIPS-FEI, The Netherlands and Tecnai G2 F30, FEI, Eindhoven, The Netherlands respectively). The TEM-EDS spectrum of the reacted Pd/Fe nanoparticles supported on mesoporous silica was obtained on an energy-dispersive X-ray spectrometer combined with the transmission electron microscope. The samples for TEM analysis were dispersed in absolute ethanol and then dropped onto TEM grids coated by carbon film prior to being mounted into the instrument.

4.2.4. Degradation and Dechlorination of Trichloroethylene

Batch experiments were carried out in 25 mL headspace bottles. Different reactors were prepared for each sampling point. A 10 mL suspension of Pd/Fe nanoparticles supported on mesoporous silica or bare Pd/Fe nanoparticles and a 0.5 mL stock solution of trichloroethylene (1.90×10^{-3} mmol of trichloroethylene) were added into the reactors. The resultant concentration of trichloroethylene was 23.7 mg/L (0.181 mmol/L). For the two supported Pd/Fe nanoparticles, the loading of iron was 203 mg/L (3.63 mmol/L), corresponding to an amount five times what is needed stoichiometrically to transform trichloroethylene into ethane completely; and the loading of mesoporous silica was 8.10 g/L. The bare Pd/Fe nanoparticles with the weight percentage of palladium to iron at 0.075% were loaded at the same iron loading as the two supported Pd/Fe nanoparticles. The bare Pd/Fe nanoparticles with the weight percentage of palladium to iron at 0.10% were added at an iron loading of 1.91×10^3 mg/L (34.2 mmol/L), which is 47 times the stoichiometric amount needed to convert trichloroethylene into ethane. The reactors were capped with butyl rubber septa wrapped by Teflon tape and sealed with flip-off caps by a hand crimper, followed by being placed upside down in a thermostatic oscillator (HZQ-F160, Harbin Donglian Electronic technology Development, Haerbin, China) and shaken horizontally at 130 r/min and 25 °C. A 200 μL of headspace sample was withdrawn from a separate reactor with a pressure-lock syringe (pre-equilibrated with the oscillator temperature) at each selected time interval while the reactor was still inside the oscillator. Then the reactor was discarded from the oscillator.

4.2.5. Sample Analysis

Headspace samples were injected with a split ratio of 10 at 230 °C into a GC (2014C, Shimadzu, Kyoto, Japan) equipped with a HP-PLOT Q column (Agilent, Santa Clara, CA, USA) (30 m × 0.32 mm × 20 μm) and a FID (flame ionization detector). The oven temperature was initially kept at 50 °C for 2 min, then heated to 220 °C at a ramp rate of 15 °C/min and held at 220 °C for 6 min. The carrier gas was high purity nitrogen at a flow rate of 2 mL/min. The temperature of the FID was set at 250 °C. Trichloroethylene, ethylene and ethane were quantified with the calibration curves. The calibration curve of trichloroethylene was obtained by analyzing the headspace gas which is equilibrated with the standard solutions of trichloroethylene under the same conditions as the reaction. The reference gas samples of ethylene and ethane were introduced into the GC through a six-port valve. The concentration of ethane and ethylene in reactors were calculated based on the assumption that they were released into the headspace completely.

Acknowledgments: This research was financially supported by National Natural Science Foundation of China (Project No. 20807004) and General Research and Development Funding for Universities directly under the Ministry of Education of PR China (Project No. BUCT-ZZ1202).

Author Contributions: Jianjun Wei, Yajing Qian and Lutao Wang conceived and designed the experiments. Yajing Qian, Lutao Wang, Yijie Ge, Lingyan Su, DebinZhai, Jiang Wang, and Jing Wang performed the experiments. Jianjun Wei, Yajing Qian, Lutao Wang and Jiang Yu analyzed the data. Jianjun Wei wrote the paper.

Conflicts of Interest: The authors declare no conflict of interest. The funding sponsors had no role in the design of the study; in the collection, analyses, or interpretation of data; in the writing of the manuscript, and in the decision to publish the results.

Appendix

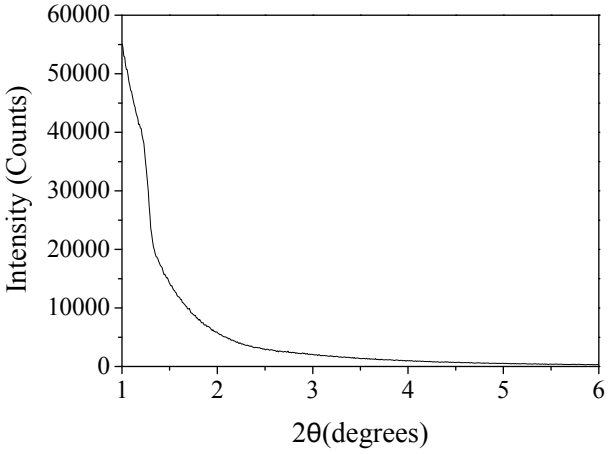

Figure A1. Low-angle XRD pattern of mesoporous silica.

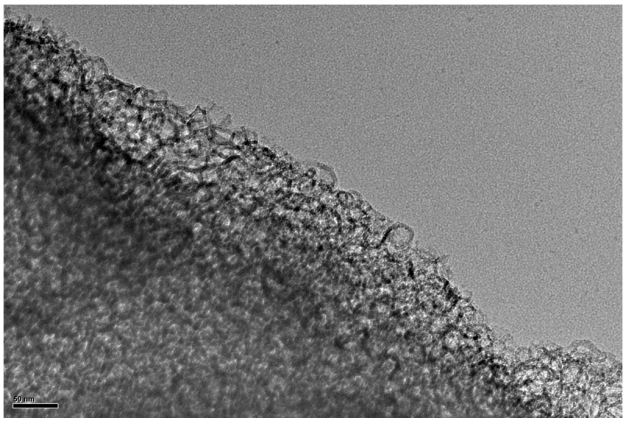

Figure A2. TEM image of mesoporous silica.

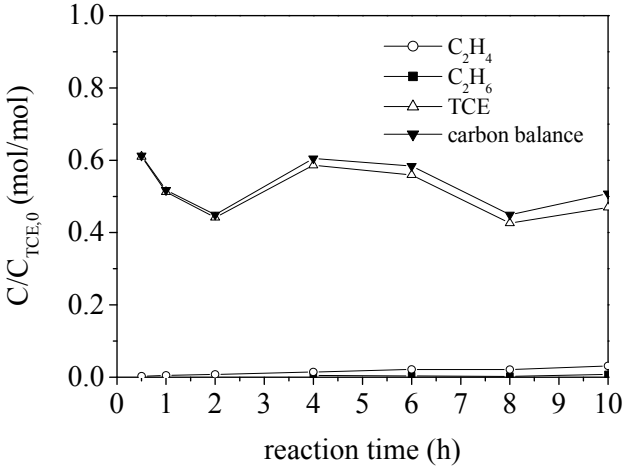

Figure A3. Degradation of trichloroethylene and production of ethylene and ethane on Pd/Fe nanoparticles supported on mesoporous silica with a weight percentage of Pd to Fe at 0.050%.

References

1. Chun, L.C.; Baer, D.R.; Matson, D.W.; Amonette, J.E.; Penn, R.L. Characterization and reactivity of iron nanoparticles prepared with added Cu, Pd, and Ni. *Environ. Sci. Technol.* **2010**, *44*, 5079–5085. [CrossRef] [PubMed]
2. Tee, Y.H.; Bachas, L.; Bhattacharyya, D. Degradation of trichloroethylene by iron-based bimetallic nanoparticles. *J. Phys. Chem. C* **2009**, *113*, 9454–9464. [CrossRef] [PubMed]
3. Yan, W.L.; Lien, H.L.; Koel, B.E.; Zhang, W.X. Iron nanoparticles for environmental clean-up: Recent development and future outlook. *Environ. Sci. Process. Impacts* **2013**, *15*, 63–77. [CrossRef] [PubMed]
4. Zhang, W.H.; Quan, X.; Wang, J.X.; Zhang, Z.Y.; Chen, S. Rapid and complete dechlorination of PCP in aqueous solution using Ni-Fe nanoparticles under assistance of ultrasound. *Chemosphere* **2006**, *65*, 58–64. [CrossRef] [PubMed]
5. Zhu, B.W.; Lim, T.T. Catalytic reduction of chlorobenzenes with Pd/Fe nanoparticles: Reactive sites, catalyst stability, particle aging, and regeneration. *Environ. Sci. Technol.* **2007**, *41*, 7523–7529. [CrossRef] [PubMed]
6. Colombo, A.; Dragonetti, C.; Magni, M.; Roberto, D. Degradation of toxic halogenated organic compounds by iron-containing mono-, bi- and tri-metallic particles in water. *Inorg. Chim. Acta* **2015**, *431*, 48–60. [CrossRef]
7. Choi, H.; Al-Abed, S.R.; Agarwal, S.; Dionysiou, D.D. Synthesis of reactive nano-Fe/Pd bimetallic system-impregnated activated carbon for the simultaneous adsorption and dechlorination of PCBs. *Chem. Mater.* **2008**, *20*, 3649–3655. [CrossRef]
8. Sunkara, B.; Zhan, J.J.; Kolesnichenko, I.; Wang, Y.Q.; He, J.B.; Holland, J.E.; McPherson, G.L.; John, V.T. Modifying metal nanoparticle placement on carbon supports using an aerosol-based process, with application to the environmental remediation of chlorinated hydrocarbons. *Langmuir* **2011**, *27*, 7854–7859. [CrossRef] [PubMed]
9. Zhan, J.J.; Kolesnichenko, I.; Sunkara, B.; He, J.B.; McPherson, G.L.; Piringer, G.; John, V.T. Multifunctional iron-carbon nanocomposites through an aerosol-based process for the in situ remediation of chlorinated hydrocarbons. *Environ. Sci. Technol.* **2011**, *45*, 1949–1954. [CrossRef] [PubMed]
10. Li, Y.C.; Li, T.L.; Jin, Z.H. Stabilization of Fe^0 nanoparticles with silica fume for enhanced transport and remediation of hexavalent chromium in water and soil. *J. Environ. Sci.* **2011**, *23*, 1211–1218. [CrossRef]
11. Zheng, T.H.; Zhan, J.J.; He, J.B.; Day, C.; Lu, Y.F.; Mcpherson, G.L.; Piringer, G.; John, V.T. Reactivity characteristics of nanoscale zerovalent iron-silica composites for trichloroethylene remediation. *Environ. Sci. Technol.* **2008**, *42*, 4494–4499. [CrossRef] [PubMed]
12. Kresge, C.T.; Leonowicz, M.E.; Roth, W.J.; Vartuli, J.C.; Beck, J.S. Ordered mesoporous molecular sieves synthesized by a liquid-crystal template mechanism. *Nature* **1992**, *359*, 710–712. [CrossRef]
13. Yuranov, I.; Moeckli, P.; Suvorova, E.; Buffat, P.; Kiwi-Minsker, L.; Renken, A. Pd/SiO_2 catalysts: Synthesis of Pd nanoparticles with the controlled size in mesoporous silicas. *J. Mol. Catal. A Chem.* **2003**, *192*, 239–251. [CrossRef]
14. Asefa, T.; Tao, Z.M. Biocompatibility of mesoporous silica nanoparticles. *Chem. Res. Toxicol.* **2012**, *25*, 2265–2284. [CrossRef] [PubMed]
15. Zhao, D.Y.; Huo, Q.S.; Feng, J.L.; Chmelka, B.F.; Stucky, G.D. Nonionic triblock and star diblock copolymer and oligomeric surfactant syntheses of highly ordered, hydrothermally stable, mesoporous silica structures. *J. Am. Chem. Soc.* **1998**, *120*, 6024–6036. [CrossRef]
16. Qiu, X.H.; Fang, Z.Q.; Liang, B.; Gu, F.L.; Xu, Z.C. Degradation of decabromodiphenyl ether by nano zero-valent iron immobilized in mesoporous silica microspheres. *J. Hazard. Mater.* **2011**, *193*, 70–81. [CrossRef] [PubMed]
17. Zhang, R.M.; Li, J.S.; Liu, C.; Shen, J.Y.; Sun, X.Y.; Han, W.Q.; Wang, L.J. Reduction of nitrobenzene using nanoscale zero-valent iron confined in channels of ordered mesoporous silica. *Coll. Surf. A Physicochem. Eng. Asp.* **2013**, *425*, 108–114. [CrossRef]
18. Sun, X.; Yu, H.X.; Zheng, D.; Wang, X.S.; Li, J.S.; Wang, L.J. Incorporation of nanoscale zero-valent iron particles inside the channels of SBA-15 silica rods by a "two solvents" reduction technique. *Appl. Surf. Sci.* **2013**, *279*, 1–6. [CrossRef]
19. Sing, K.S.W.; Everett, D.H.; Haul, R.A.W.; Moscou, L.; Pierotti, R.A.; Rouquérol, J.; Siemieniewska, T. Reporting physisorption data for gas/solid systems with special reference to the determination of surface area and porosity (Recommendations 1984). *Pure Appl. Chem.* **1985**, *57*, 603–619. [CrossRef]

20. Schmidt-Winkel, P.; Lukens, W.W., Jr.; Zhao, D.Y.; Yang, P.D.; Chmelka, B.F.; Stucky, G.D. Mesocellular siliceous foams with uniformly sized cells and windows. *J. Am. Chem. Soc.* **1999**, *121*, 254–255. [CrossRef]
21. Taghavimoghaddam, J.; Knowles, G.P.; Chaffee, A.L. Preparation and characterization of mesoporous silica supported cobalt oxide as a catalyst for the oxidation of cyclohexanol. *J. Mol. Catal. A Chem.* **2012**, *358*, 79–88. [CrossRef]
22. Liu, J.; Li, C.M.; Yang, Q.H.; Yang, J.; Li, C. Morphological and structural evolution of mesoporous silicas in a mild buffer solution and lysozyme adsorption. *Langmuir* **2007**, *23*, 7255–7262. [CrossRef] [PubMed]
23. Lien, H.L.; Zhang, W.X. Nanoscale Pd/Fe bimetallic particles: Catalytic effects of palladium on hydrodechlorination. *Appl. Catal. B Environ.* **2007**, *77*, 110–116. [CrossRef]
24. Schrick, B.; Blough, J.L.; Jones, A.D.; Mallouk, T.E. Hydrodechlorination of trichloroethylene to hydrocarbons using bimetallic nickel-iron nanoparticles. *Chem. Mater.* **2002**, *14*, 5140–5147. [CrossRef]